








Seismic risk analysis of a data communication network

Simona Esposito^a, Alessio Botta ^b, Melania De Falco ^c, Adriana Pacifico^d, Eugenio Chioccarelli ^e,
Antonio Pescapè ^b, Antonio Santo^c and Iunio Iervolino ^d

^aSwiss Re Management Ltd, Zurich, Switzerland; ^bDipartimento di Ingegneria Elettrica e delle Tecnologie dell'Informazione, Università degli Studi di Napoli Federico II, Naples, Italy; ^cDipartimento di Ingegneria Civile, Edile e Ambientale, Università degli Studi di Napoli Federico II, Naples, Italy; ^dDipartimento di Strutture per l'Ingegneria e l'Architettura, Università degli Studi di Napoli Federico II, Naples, Italy; ^eDipartimento di Ingegneria Civile, dell'Energia, dell'Ambiente e dei Materiali, Università degli Studi Mediterranea di Reggio Calabria, Reggio Calabria, Italy

ABSTRACT

Data communication networks have large importance for the immediate post-earthquake emergency management and community resilience. In this study, the framework of simulation-based probabilistic seismic risk analysis of data communication infrastructure is applied to the real case of the inter-university data network of the Campania region (southern Italy). The network is constituted by point-like facilities (racks located within buildings and containing the device routing and managing traffic) and distributed links (buried fiber optic cables). The seismological, geological, and geotechnical features of the region were characterized together with the seismic vulnerability of each element of the network. The network performance is quantified in terms of traffic loss before and after the seismic event. Results are provided in terms of annual rate of events exceeding traffic loss thresholds and allow to identify the portion of the network mostly contributing to the seismic performance.

ARTICLE HISTORY

Received 29 August 2020
Accepted 1 November 2021

KEYWORDS

Civil infrastructure system; performance-based earthquake engineering; failure recovery mechanisms; regional seismic hazard; fragility functions; seismic losses

1. Introduction

Civil engineering research is dealing, among topics of largest interest nowadays, with resilience to natural hazards of systems and assets serving the communities of the region where they are deployed. Resilience is intended as the set of attributes that allows the continuity and/or the restoration of the everyday life and business quality after a disrupting event. In fact, when it comes to earthquake engineering, there is a significant deal of research focusing on risk assessment of single utility distribution systems, as gas or electric networks (e.g., Esposito et al., 2015; Cavalieri et al., 2014a; Chang & Wu, 2011; Lanzano et al., 2014; D'onofrio et al., 2013; Ningxiong et al., 2007) and transportation networks (e.g., Argyroudis et al., 2015; Chang et al., 2012; Forte et al., 2015; Kiremidjian et al., 2007); in some cases, the interdependency of critical networks is also considered (e.g., Duenas-Osorio et al., 2007; Omidvar et al., 2014; Poljanšek et al., 2012). The study by Esposito et al. (2015) attempted to extend the probabilistic paradigm of performance-based earthquake engineering or PBEE (Cornell & Krawinkler, 2000), originally developed for buildings (i.e., point-like structures), to spatially distributed systems. PBEE entails the probabilistic characterization of (1) the seismic hazard, (2) the system's

vulnerability, and (3) the consequences of the seismic damage to the structure/system of interest (i.e., the losses). Each of these three items presents scientific and practical challenges when dealing with distributed infrastructure that motivate the mentioned research effort. Moreover, even in the broader PBEE framework adapted to spatial systems, each infrastructure requires specific calibration of the hazard, vulnerability, and loss models that reflect the peculiarities of the physical assets and of the consequences of seismic damages to them. The final aim is to compute the expected annual performance loss for seismic causes, so as to be able to check its tolerability and eventually direct risk mitigation resources.

Telecommunication networks (i.e., landline-voice, wireless-cellular, and data communication networks) can be certainly framed in the context of utility systems, and among those of largest importance for the immediate post-event emergency management and community resilience. Hence, following a lifeline disrupting event, the demand for telecommunication services may increase, often exceeding the capacity of these networks. On the other hand, these systems seem relatively less studied (in the earthquake engineering community) with respect to those mentioned above, although a few

attempts exist (e.g., Leelardcharoen, 2011). It has also to be mentioned that the documented behavior of these systems in recent damaging events was quite well described. Failures of some components were still found, especially on building-type components and equipment. To give some examples, the moment magnitude, M_w , 8 Mexico City earthquake in 1985 had collapsed three floors of a communications building (Tang, 2008). The Technical Council of Lifeline Earthquake Engineering (TCLEE) analyzed damages in the nodes and links of the telecommunication networks caused by both the M_w 7.1 4 September 2010 and the M_w 6.3 22 February 2011 New Zealand events (TCLEE, 2012): it was observed that there was a variety of damage to underground facilities due to soil liquefaction. From a systemic point of view, instead, telecommunication networks have been performing well during the short-term post-earthquake phase (Tang, 2014; TCLEE, 2011). In the 2011 M_w 9.0 Tohoku earthquake, the overall system performance of the telecommunication networks, including recovery and emergency response, was considered satisfactory particularly for the data communication network. In this case, the damages experienced by the telephone network, mainly in central offices close to the coast, were mostly due to the tsunami and power outage. However, there are other examples where earthquakes had a great impact on the performance of data communication networks, e.g., the M_w 7 Taiwan earthquake in 2006 reduced China's internet access capacity by 74% for several minutes due to fiber cables breaks. Such a capacity was progressively recovered in the following minutes due to automatic traffic reroute and in the following hours thanks to manual traffic reroute (Kitamura et al., 2007), helping the resilience of the community.

From the scientific literature on data or computer communication, it emerges that assessing the effects of earthquakes on telecommunication networks, especially the data communication networks, is an emerging topic, presenting inherent difficulty due to nature of these systems and due to the mechanisms they employ to recover from failures. Studies, focused on the evaluation of the post-event performance of these systems, showed how natural events can cause severe service network disruption. Cetinkaya and Sterbenz (2013) presented a general classification of network failures, in which they consider large-scale disasters, including earthquakes. Cho et al. (2011) analyzed the same outage on a different network. They emphasized the importance of redundancy and over-provisioning in the network design as well. Cho et al. (2011) also investigated the impact of an earthquake on a Japanese internet service provider (ISP) named IJ. Fukuda et al. (2011) analyzed the impact of

the recent Tohoku earthquake on a national network. They observed that, even though some physical links were damaged, the network connectivity was maintained thanks to physical and internet protocol (IP) level redundancy. The former is warranted by dual physical links that route along different geographical paths, whereas the latter is provided by redundant multiple loops in the network topology. Fukuda et al. (2011) investigated the earthquake impact on a different Japanese ISP named SINET4. They also used routing information and traffic volumes, logging the event messages generated by routers. Liu et al. (2012) characterized the inter-domain re-routing occurred after the 2011 Tohoku earthquake. The authors observed that three major providers of inbound traffic to Hong Kong were affected by unstable routing due to a cable fault after the earthquake. Finally, Bischof et al. (2011) gained insights into the impact of this earthquake mainly relying on measurements performed by a widely adopted peer-to-peer system (i.e., BitTorrent), identifying the specific regions and network links where internet usage and connectivity were most affected. Despite the work done, these studies do not include in their investigation the study of the physical effects of the earthquake on each component of the network, ignoring then the seismic source characterization, the wave propagation, the site amplification effects, and the seismic response behavior of each component of the network.

The scope of the study reported in this paper is to investigate the application of the performance-based seismic risk assessment adapted to spatially distributed infrastructure recently developed (e.g., Ptilakis et al., 2014) to data communication networks. In fact, this approach requires the characterization of the seismic source in terms of the stochastic process of earthquake occurrence as well as the definition of the probabilistic distributions of magnitude and location of each seismic event. Once the event is defined in terms of these characteristics, the random field of a set of ground motion intensities has to be realized for the region where the network is located. The realization of the random field is the input for the vulnerability models of network components, which in turn serve to probabilistically define the performance loss for the system under study, in the case of the considered seismic event.

The assets (i.e., components) of recent data communication networks are typically optical fibers either buried and/or running on aerial lines, as well as a number of points of presence (POPs) containing the intermediate devices, routing and managing traffic, often cased in buildings. Consequently, a data network is vulnerable to either ground shaking (transient ground deformation, *TGD*, hazard) mainly for damages of POPs, or

ground failure (i.e., geotechnical effects or permanent ground deformation, *PGD*, hazard) that are likely to damage buried lines and requires characterization of the susceptibility of the region to landslides and liquefaction. The system vulnerability to transient and permanent deformation is common to other mainly buried systems such as gas and water distribution networks. From the system's performance point of view, the metric has to be representative of the delivered traffic (often measured in bytes), given the physical status of the network before and after the seismic event.

To discuss all these issues in practice, a real case is addressed, that is, the recently established RIMIC network (*Rete di Interconnessione Multiservizio Interuniversitaria Campana*), in southern Italy. It links the universities in the Campania region and is connected, via one of its points of presence, to the nationwide GARR (*Gruppo per l'Armonizzazione delle Reti della Ricerca*) backbone. The optical fibers of RIMIC are mostly buried and the POPs are located in university buildings. Although RIMIC has several sub-networks, for the sake of simplicity, only the main loop, featuring four POPs, is considered. It deploys over more than 280 km, running in areas susceptible to ground failure and also close to the seismically active Irpinia (southern Apennines) area, which, in 1980, originated a Mw 6.9 earthquake, the most damaging in the contemporary era in Italy.

The remainder of the paper is structured such that the peculiarities of data communication networks and communication mechanisms are described in order to

understand how these networks work in normal operation status as well as during a failure. Subsequently, the general process of the performance-based seismic risk analysis for data network is described. In the second part of the paper, the RIMIC test case is described from a logical and physical point of view. The seismological, geological, and geotechnical features of the region where the system is located are described. Then, the vulnerability models adopted are discussed, as well as the algorithms to compute the performance loss in the case of a seismic event. All these components are tied together and the seismic risk assessment for RIMIC is carried out.

2. Data communication networks

A data communication network can provide connectivity between individual networks (i.e., telecommunication companies, multiple service providers and end nodes) at various levels through a complex and hierarchical interconnection of nodes and links. As schematically shown in Figure 1, computers at the border of the network (also called end-hosts; i.e., devices used by human beings, servers, data centers, machines performing automated tasks, and, in general, all the entities that use the network for data communication with other entities) are connected through a series of intermediate devices (mainly switches and routers) that route, reroute, and in general, manage the traffic. From a physical point of view, the typical structure of a

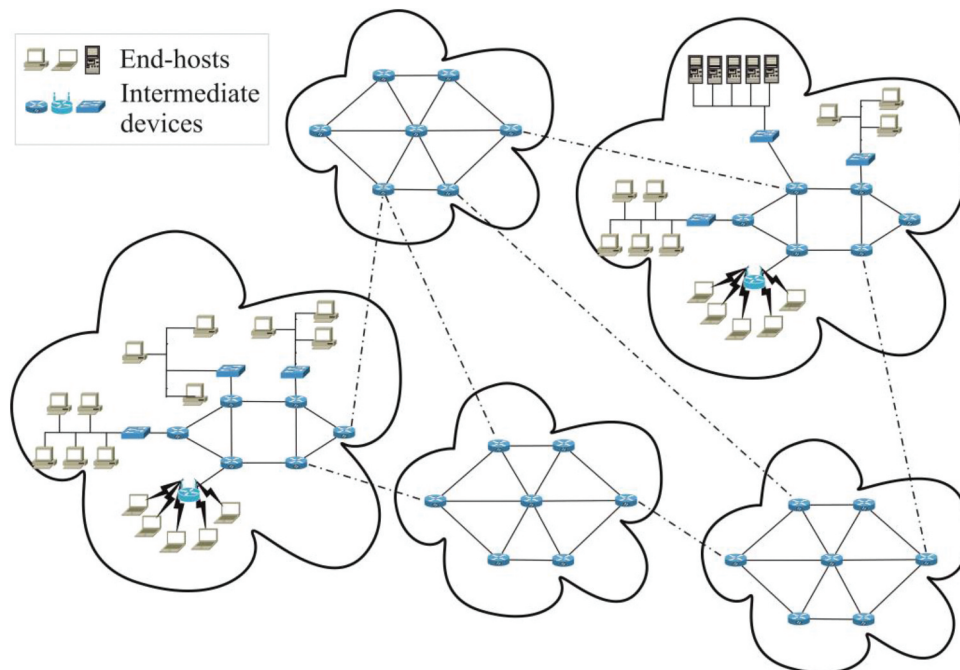


Figure 1. Example of individual data networks with interconnections.

communication network is then composed of a number of point-like facilities (i.e., the intermediate devices) and distributed links (mainly fiber optics or copper cables) either buried and/or running on aerial lines. The intermediate devices usually reside inside the POPs that represent the principal points of concentration and distribution of connectivity of the network. POPs are usually located in building facilities that provide appropriate services (electricity, air conditioning, alarm systems, fire protection, etc.) to ensure continuous operation of the devices and the proper installation of suitable racks to house such devices. Each rack contains optical adds/drop multiplexer, switches, routers, and, in general, all the devices needed to handle the traffic of the network.

Large networks are often organized in a hierarchy, where the highest level forms a backbone for the other levels. Today, each level of a geographical network is typically organized as a loop, where at least two cables connect each POP to other two POPs of the same level. This is to ensure that all the POPs have different paths available, which is an important redundancy requirement, especially for the main loops. POPs of lower layers are then possibly connected to, at least, one POP of the higher layer and to another POP of the same level.

2.1. Communication mechanism

The information exchanged between the end-hosts (e.g., a web page, an image, or a voice flow) is fragmented in a number of pieces called packets. Each of these packets is then transmitted through the network, where each of the intermediate devices does packet switching; i.e., receives the packet first, inspects some part of the packet content (e.g., to find the intended destination), and finally forwards it through a specific link to a certain next intermediate device or to the destination end-host. All such packets constitute the so-called network traffic, which is therefore flowing on the links of the network, handled by the intermediate devices, and coming from and going to all the possible end-hosts in the network.

All the hosts of these network (end-host and intermediate devices) use a very simple protocol to exchange data; i.e., the IP. This protocol is connectionless and best effort, in the sense that it tries to deliver each new packet produced by the application at its destination using the route available in that moment. However, it does not guarantee that packets are actually received by the destination. Upper-layer protocols working on top of the IP are in charge of verifying if the packets have been received by the destination and retransmitting them in case of loss. On the other hand, intermediate devices have several links of different kinds (fiber optics, copper

cables, wireless links, etc.) and several possible paths among them and perform an important function on packets, generally called routing. Basically, on packets arrival from a certain source on a certain link, they have to decide where to forward these packets, in order for them to arrive to their destination. To do this, they construct the so-called routing tables; i.e., tables containing the outgoing link to be used for each possible destination. These tables are constructed by each device at start-up and continuously updated using the so-called routing protocols, which are based on the exchange of specific information among them.

2.2. Failure-recovery mechanisms

A key feature of data distribution networks are failure-recovery mechanisms. They can be of two main classes, depending on the layer of the protocol stack they operate at: *IP-layer* and *physical-layer*.

IP-layer mechanisms (also called routing-layer mechanisms) are realized by routing-algorithms performed by the intermediate devices (the routers in particular). These devices, in case of link and node failures, may be able to automatically find a new path towards the destination through a process called re-routing. The time required for the IP-layer mechanisms to reach the new stable configuration and to deliver previously lost packets can be in the order of several minutes because network-layer devices require to exchange several messages in order to find the new paths. The actual time depends on several factors such as the internal state of the routing protocol, the topology and configuration of the network, the complexity of the network, the available paths that survived the failure, the routing protocol, etc.

Physical-layer mechanisms operate differently. In case two or more links connect two physical layer devices (e.g., more optical fibers within the same cable), if the primary link breaks, another one is automatically activated without the need for external actions and without informing all the other devices. Thus, the connection between the two devices remains functional. These mechanisms may recover from failures in a much shorter time with respect to the IP-layer ones. However, they can be of help only if a part of, but not all, the cables connecting the devices is broken.

3. Performance-based seismic risk analysis of data communication networks

Recently, there has been a significant body of research focusing on risk assessment of infrastructural systems, aimed at extending the fully probabilistic paradigm of

PBEE to distributed systems (Pitilakis et al., 2014). The PBEE framework seems to be applicable also to data networks benefitting from similar research on different systems; however, the models for the seismic performance evaluation are network-specific and require further developments.

This section describes first the general process to characterize the seismic hazard acting on the components of a data communication network. Then, the characterization of seismic vulnerability of each component and the performance of the network as a whole is reviewed, highlighting the principal differences and limitations with respect to single-site systems.

3.1. Seismic hazard characterization

A data communication network is a spatially distributed system made of different components. This means that the seismic hazard of the region where the network is located has to be evaluated jointly for all the locations of the system's components (e.g., Weatherill et al., 2014). Moreover, the joint evaluation of different ground motion intensity measures (IMs), that serve as input for the vulnerability models of the different components, is required. These aspects represent the key difference with respect to seismic risk analysis of point-like facilities. Indeed, besides the characterization of the seismic source in terms of earthquake occurrence, geometry, fault (i.e., the seismic rupture) mechanism, and other source parameters and the probabilistic distribution of magnitude and location of each seismic event, the seismic hazard has to be represented in terms of random fields accounting for the statistical dependencies between different ground motion parameters at different sites in the same event. Thus, the probabilistic seismic input representation has to account for both the *spatial-correlation* (e.g., Esposito & Iervolino, 2011) and the so-called *cross-correlation* (e.g., Loth & Baker, 2013) among the IMs.

The last aspect to consider in the characterization of the seismic hazard of data networks is that, the presence of buried components (i.e., cables), if any, generally requires the consideration of *PGD* hazard (triggered by *TGD*), such as landslides, liquefaction, and fault displacements (Kramer, 1996). The *PGD* hazard depends on several factors related to the geological/geotechnical conditions of the subsoil. In general, co-seismic fault displacement is evaluated by means of semi-empirical relations that correlate displacement to the magnitude of the earthquake (e.g., Petersen et al., 2011). For liquefaction and seismic-induced landslide hazard, many models relate the permanent displacement and its occurrence probability to transient ground motion

parameters, typically the peak ground acceleration, *PGA*, or the peak ground velocity, *PGV*, e.g., O'Rourke and Palmer (1996). Among the different approaches proposed in literature, the simple approach of HAZUS (FEMA, 2004) represents a base-level scale-compatible application of geotechnical hazard characterization in the context of probabilistic seismic risk analysis of spatially distributed systems (e.g., Esposito et al., 2015), since it requires limited information about the geotechnical characterization of the region.

3.2. Characterization of seismic vulnerability

To assess seismic damage of each component of a data network given ground shaking or ground deformation hazard, IMs have to be related to the effects by means of models, e.g., the *fragility* functions. In particular, for point-like systems, these relations typically provide the probability of reaching or exceeding a damage state (DS) given the intensity. At the lowest refinement level, the vulnerability characterization of POPs may be performed analyzing the seismic behavior of the hosting facility (i.e., buildings) and the equipment inside (i.e., presence of anchored or unanchored subcomponents or electrical components, connection type, etc.).

Regarding the distributed elements, cables are usually made of fiber optics or copper and they can be either buried and/or running on aerial lines. While aerial lines are usually relatively less prone to damage (Adachi & Ellingwood, 2008; Cavalieri et al., 2014b), buried cables can be damaged during earthquake being (in principle) sensitive to both *TGD* and *PGD*. Usually a repair rate, *RR*, that is the expected number of damages per unit length of the buried link, can be defined as a function of the ground motion intensity at each site. The *RR* is considered as the rate of a Poisson process describing the occurrence of a rupture along the length of the link (*l*); e.g., Lanzano et al. (2014). Thus, the probability that the link fails, $P_f[link(l)]$, that is, the probability that at least one rupture occurs on the link, is equal to

$$P_f[link(l)] = 1 - e^{-RR \cdot l} \quad (1)$$

3.3. Systemic performance and risk

Performance evaluation of infrastructure systems reflects their spatially distributed and functionally interconnected nature, which needs specific indicators (Cavalieri et al., 2014a; Esposito et al., 2015; Franchin & Cavalieri, 2013). The identification and description of the relation/interactions between the components of each system (intra-dependencies) and inter-relations

between the systems (inter-dependencies) is a fundamental step for the evaluation of the state of the system (i.e., the performance) as a function of the states of its components and of other systems. The quantitative measure of the performance of the whole system and its elements is usually given by performance indicators (PIs). PIs depend on the type of analysis that is performed on the network. In particular, two types of system evaluation may be considered: (1) *connectivity analysis* and (2) *capacity analysis*.

- (1) *Connectivity analysis* is related to the existence of a path connecting sources to demand nodes (in a system where both links and nodes may fail) requiring a simple description of the system in terms of a graph and the application of graph algorithms to evaluate the connectivity and the accessibility of nodes (Duenas-Osorio et al., 2007).
- (2) *Capacity analysis* requires graph algorithms and flow equations that are used to estimate capacitive flows from sources to end nodes based on the damages sustained by the network components (e.g., Nuti et al., 2009; Vanzi, 2000).

Differently from the connectivity analysis that relies only on the use of graph algorithms, applicable to all kind of networks, the capacity analysis requires more refined and network-dependent approaches. In the case of data networks, this requires the knowledge of the amount of traffic flowing through the network that can be viewed at different levels of aggregation (i.e., the total on the network, the amount on each link, etc.). Such amount of traffic is dependent on the number and kind of users, applications, and end-hosts on the network, but it is also strongly dependent on the characteristics of the network in terms of capacity to actually transport such traffic to its intended destination. Therefore, the traffic on the network before and after the event can be used as a performance parameter to evaluate the effect of the earthquake on the network. To do this, the traffic matrix of the network before the event has to be considered first. Such matrix basically contains the volume of traffic exchanged by any two nodes in the network. Having such matrix before the event, what changes in the network after the event has to be studied.

A more fine-grained approach may consider performance parameters related to each individual traffic flow, before and after the seismic event. In more detail, performance parameters for networks using the packet switching paradigm can also be related to the number of single packets that are transmitted from a source to a destination in a certain time period (i.e., the

throughput), the amount of such packets that are lost, and the time it takes for these packets to reach their destination (i.e., the delay or latency). Such parameters can easily change after an event and analyzing their variation can provide more detailed information. For example, if a certain path of the network goes down because of an earthquake, but all the end-hosts are still connected (i.e., there are paths available among them), the network is fully connected, and the traffic loss is zero. However, the paths that are still working are now carrying more traffic than before the event. Therefore, packets going through such more congested path will experience worse conditions (e.g., more delay), and this can have an impact on the quality perceived by the users (the so-called quality of experience).

4. The regional inter-university data network RIMIC

4.1. Logical description

The network under study is an infrastructure recently deployed in the Campania Region of Italy as part of a publicly financed project called *Rete di Interconnessione Multiservizio Interuniversitaria Campana*. The project has created a high-speed and high-redundancy network connecting the universities, research centers, and public institutions of the region. The purpose of the project, and then of the network, is to build and operate, in full autonomy and total independence from private providers, an infrastructure that can ensure communication and cooperation, as well as the provision of value-added services for all the research and administration facilities located in major urban areas, to pool existing assets through the interconnection and upgrading of existing metropolitan area networks (MANs). The network is meant to be used for several services such as data communications among the served sites as well as towards the internet. It covers the entire territory of Campania, touching all the universities as well as several other research centers, public institutions, etc. Physically, the network is configured as a ring system: the first ring (or loop), shown in Figure 2, has regional coverage to which additional rings are connected to cover the MANs of the institutions in four provinces of the Campania region: Naples (NA), Caserta (CE), Benevento (BN), and Salerno (SA). RIMIC has several sub-networks, however, for simplicity, only the main loop is considered in this study. It is meant to be a backbone interconnecting the main POPs.

The secondary loops as well as other networks (e.g., the network of private operators willing to setup an exchange point with the network) are then attached to

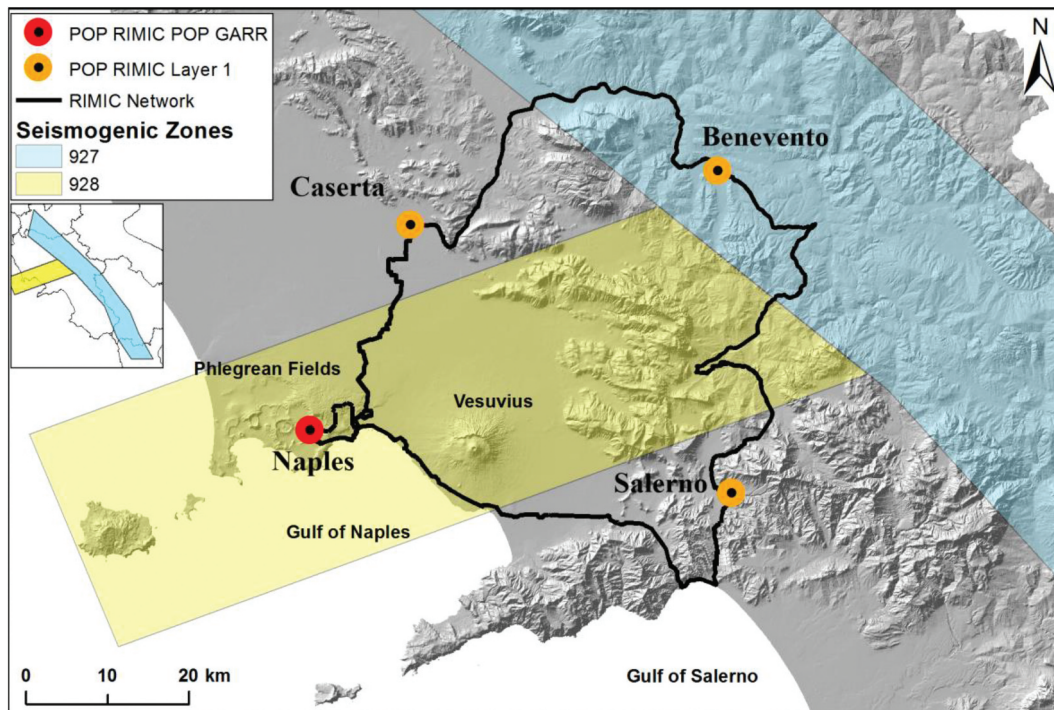


Figure 2. Map representing the main loop of the RIMIC network and its POPs together with the areal seismic source zones considered in the study.

these main POPs. POPs are also used to connect the large MAN infrastructure already developed (or in progress) by the universities and research centers as well as other public and private networks. In practice, POPs act as hubs concentrating and distributing connectivity to the networks of research, teaching, or administration institutions. Regardless of the hierarchical level of membership, all POPs also perform aggregation of connections of end-hosts. In particular, these hosts can be connected in two different modes:

- directly connected to the nearest POP via optical fiber;
- connected through urban and/or regional networks connected to the POP.

The hierarchical structure of the network ensures high availability: the nodes of the main loop have at least two paths geographically diversified. Such dual path connection is meant to manage network failures by dynamically re-directing traffic on the alternative route. In addition to that, network devices inside POPs are inherently redundant, decoupling the transmission components of the different optical fibers so as to cope with failures of such components. The network has *physical- and IP-layer recovery mechanisms*. First, each physical link is realized through different couples of optical fibers, and physical-layer mechanisms are then adopted to automatically reroute traffic on the

backup fiber in case of failure of the primary one. Moreover, the loop structure allows redundancy, and thus protection, also in case POPs or paths connecting POPs fail (e.g., rupture of the entire cable containing all the optical fibers). In this case, automatic and dynamic rerouting is performed.

Routing is based on the combination of two protocols: open shortest path first (OSPF), used for the internal reachability of the backbone, and border gateway protocol (BGP), used for the propagation of the routes regarding external networks. BGP is configured on all the routers in the first-level POPs and the edge routers of the external networks. Routes in the first-level POPs are also set as route reflector and have a full mesh of internal BGP sessions between them. The functionality of the route reflector is to logically divide the backbone in a set of clusters, to reduce the need of meshing of the BGP sessions to a single element of each cluster. The interior routing protocol, OSPF, is used for determining the address of the next hop router, while BGP carries the routing information of local networks to the backbone.

It should be noted that, finally, the control over all levels of the protocol stack implemented in this network allows the choice of the level at which to enable the protection mechanisms. In any case, even if in principle it is possible to simultaneously use these mechanisms at different levels of the protocol stack, due to possible instability resulting from the joint use of these strategies, mechanisms at only one level are normally operating.

4.2. Physical description

As mentioned before, the case study is composed by four main nodes (POPs) one of which (i.e., the Naples' POP, represented in red in Figure 2) is connected to the ultra-broadband national network, GARR, the network connecting universities, and research institutes in Italy. The four POPs are located in building facilities providing appropriate services and housing the racks for the devices. The racks are anchored and housed in the four buildings at the ground floor. The main characteristics of the four buildings and the corresponding vulnerability class according to HAZUS (FEMA, 2004) taxonomy are summarized in Section 5.2.1.

The four POPs are connected by a ring of about 280 km of optical fibers. The fiber optic links are mainly housed along roads (urban and extra urban), railroads, and in some parts along bridges decking systems and tunnels that create a linkage in both transportation and telecommunication networks. Fiber optic cable lines are buried at about 1 m and have a diameter of 50 mm. They are characterized by a central strength member needed to provide the rigidity to keep the cable from buckling and protect the individual fiber optic cable from breaking during the installation. The individual fiber tubes are stranded around the central member into a compact and circular cable core. Around the cable cores, there is an aluminum polyethylene laminate filled with a compound that protect the individual cables from water ingress. The cable core is then covered with a double polyethylene sheath that enhances cable crush resistance, impact resistance and moisture proofing.

4.3. Seismotectonic and geological setting

The network crosses a wide area along relevant expressways passing for the main cities of Campania region. It lies on different geological formations, eventually characterized by the presence of a groundwater level in the shallower layers, which can affect the seismic site response analysis and the occurrence of landslides and liquefaction phenomena. The study area is in the southern Apennines, a fold and thrust belt mainly made of imbricated sheeted of limestones and flysch deposits. Its formation started during the Miocene orogenesis and lasted in the whole Quaternary, when the geological setting was furtherly articulated by the extensional tectonics due to the opening of the Tyrrhenian Sea (Patacca & Scandone, 2007). Figure 3a shows the RIMIC track and the intersected geolithological complexes, mainly located in plains and riverine contexts and only in few cases along slopes (slope angles are identified in Figure 3b). The shallower layers (2–3 m depth) are constituted by pyroclastic materials, debris, paleosoils, and infillings, but for the scale of this study (1:100.000), only the geologic bedrock was considered. The concrete rigid structures (tunnels and bridges), on which the network can be located, were neglected too.

The case study area is mainly interested by two areal seismic source zones, shown in Figure 2 and Figure 3b, which are also considered in this study. They are from the Meletti et al. (2008) seismic zone model of Italy (used for the official seismic hazard map of the country; i.e., Stucchi et al., 2011). Seismological characterization of the two seismic zones is given in Section 5.1.

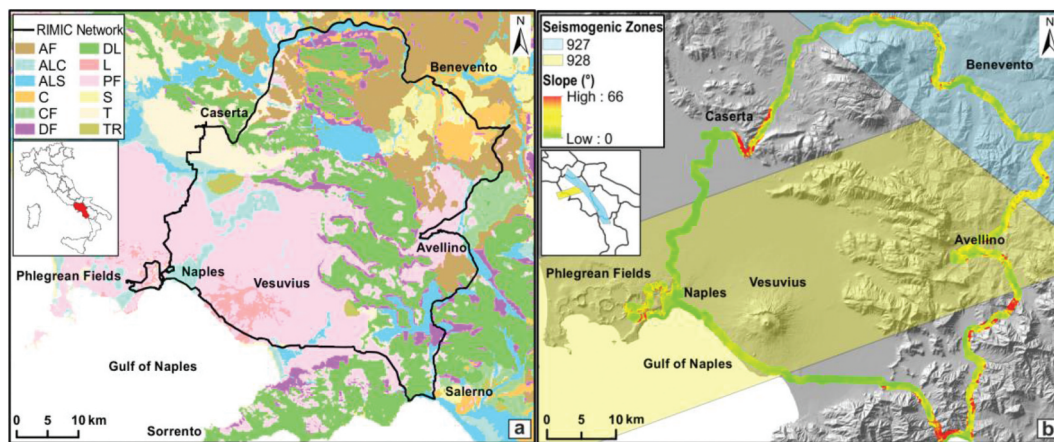


Figure 3. (a) The outcropping lithological formations: CF, clay formation; AF, arenaceous formation; DL, dolostone and limestone; C, conglomerate; S, sand; L, lava; ALC, alluvial and lacustrine clay; ALS, alluvial sand; DF, debris and fan deposits; T, tuff; PF, pyroclastic fall; TR, travertine. (b) Slope angle map with seismogenic zones.

5. Analysis

The scope of the present study is to apply the performance-based seismic risk assessment, adapted to data communication networks (discussed in Section 3), to the case study of the main loop of RIMIC network (described in Section 4). The network performance was assessed in terms of a capacity-level PI evaluating the traffic that is correctly transferred through the network to the POPs (see Section 5.3), before and after an earthquake. Both TGD and PGD hazards were accounted for. Fiber cables and POPs were the considered vulnerable elements.

The simulation was performed implementing the application network in the object-oriented framework for infrastructure modelling and simulation (OOFIMS, <https://sites.google.com/a/uniroma1.it/oofims/>, last accessed July 2020) software (Franchin & Cavalieri, 2013) for the seismic risk assessment of interconnected infrastructural systems. For the purpose of this study, the software was enhanced with the tele-communication (TLC) class that is composed of nodes and link/edges. As consequence, the TLC class is the composition of the TLCedge and TLCnode abstract classes, the first of which is the generalization of the FiberOptics class, while the second is the generalization of the POP and Pathpoint classes, as shown in Figure 4. The Pathpoint class represents all nodes used to reproduce the geometry of the network and the POP class represents the nodes used to transmit data. For each class, several methods (i.e., functions used to evaluate the state of the network and of each component) and attributes (i.e., properties that describe the whole system and each component) were defined in order to evaluate the state of the network and components.

5.1. Simulation of seismic input

The computation of the seismic input in each run of the simulation is mainly characterized by four phases: (i) simulation of an earthquake on the considered seismic

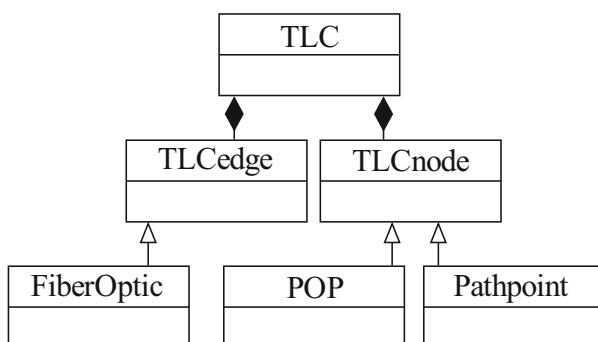


Figure 4. Class diagram for the telecommunication network.

sources; (ii) computation of the ground motion for the region where the network is located; (iii) amplification of the ground motion due to local site conditions; and (iv) computation of the ground failure displacement induced by liquefaction and landslide; see Esposito et al. (2015) for procedural details.

In each run, the seismic event is simulated in terms of earthquake location and magnitude considering the two seismic sources, named 927 and 928, of the Meletti et al. (2008) seismic model of Italy (Figure 3b). Data characterizing the seismic zones are summarized in Table 1, which is from Barani et al. (2009). The magnitude of each event is extracted from considering an exponential (truncated) distribution. It is built according to the Gutenberg-Richter relationship (Gutenberg & Richter, 1944) for the source. As a result, the source zone is characterized by minimum and maximum (surface wave) magnitude values (M_{min} and M_{max} , respectively), mean annual number of earthquakes (i.e., rate) with magnitude above M_{min} , indicated as ν , and negative slope of the Gutenberg-Richter relation, b . Given the magnitude, the simulation of the earthquake on the two seismic zones was in terms of location (i.e., the epicenter), which was assumed as uniformly distributed over each source zone. Both seismic zones are characterized by a normal prevalent fault mechanism; thus, a normal rupture is associated to all the generated events.

To discuss the performance of the network, which follows, it is here useful to note that, given that classical seismic hazard analysis (e.g., Chioccarelli et al., 2019) assumes a homogeneous Poisson process for the earthquake (mainshock) occurrence (not to be confused with the Poisson process for breaks of links in a given earthquake), the mean interarrival time between two subsequent earthquakes above the minimum magnitude considered on the sources (of any considered magnitude and location), that is the *return period*, is equal to about 2.4 years (i.e., the reciprocal of the sum of the two rates in the second column of Table 1).

The earthquake IM considered to simulate the ground motion is the PGA. This is because the fragility curves of POPs are function of PGA (see next section), while PGD in each site is derived by simulated PGA (as described in the following of this section). The PGA field at the bedrock (i.e., before propagating in the soil) for each scenario is evaluated using the Bommer et al.

Table 1. Parameters of the selected seismic sources.

Zone	ν (1/year)	b	M_{min}	M_{max}	Prevalent fault mechanism
927	0.362	0.557	4.3	7.3	Normal
928	0.054	1.056	4.3	5.8	Normal

(2012) ground motion prediction equation (GMPE) on a regular grid of points discretizing the region covered by the network, as expressed in Eq. (2):

$$\log(PGA_{ij}) = E[\log(PGA)|m_i, r_{ij}, \theta] + \eta_i + \varepsilon_{ij} \quad (2)$$

where PGA_{ij} denotes the PGA at the site j due to earthquake i ; $E[\log(PGA)|m_i, r_{ij}, \theta]$ is the expected value of its logarithm, conditional to the earthquake of known magnitude (m_i), source-to-site distance (r_{ij}), and rupture mechanism (θ); η_j is the inter-event residual, common to all sites, and assumed as a normally distributed random variable with zero mean and standard deviation σ_{inter} (from the GMPE model) to be sampled in each earthquake simulation; ε_{ij} is the intra-event (site-to-site in the same event) heterogeneity of ground motion (independent of the inter-event residual), usually modeled via a multivariate zero-mean Gaussian distribution with covariance matrix reflecting correlation as a function of inter-site distance (see Jayaram & Baker, 2009). In this case, the intra-event (spatially correlated) residual model was formulated according to Esposito and Iervolino (2011).

GMPE-based amplification factors were considered to account for local site conditions and to transform the PGA at the bedrock in the PGA at the surface (PGA_S). To this aim, a geological analysis of the region was performed and the average shear-wave velocity between 0 and 30-meters depth (V_{S30}), which is a proxy for soil response, was associated to each site of the network based on a 1:100.000 scale ISPRA geological maps (see Data and Resource section). To do that, the outcropping lithological formations (Figure 3a) were grouped in classes taking into account their similarity in lithology, facies, and diagenesis degree and each class was classified following the EUROCODE 8 (2003) categories, by means of a statistical processing of the V_{S30} values coming from available down-hole measurements (Forte et al., 2017).

Regarding the ground failure (i.e., PGD hazard), the potential earthquake-induced events which may occur in each simulated event are rock falls and debris flows along high angle calcareous slopes (southern sector of Figure 3a), reactivation of slow slope movements in the clayey hills domains (northern and eastern sector), and sandy silt soil liquefaction in the intermountain basins (northern) and alluvial plains (western sector). Therefore, the landslide and the liquefaction potential of the region, where the network is deployed, were evaluated, according to the HAZUS procedure (co-seismic surface ruptures was neglected). In particular, a landslide susceptibility map was obtained for the purpose of this study, based on the geological groups, slope

angles, and ground-water conditions of the study area. At both side of the network a buffer polygon of 500 meters was considered. The slope angle map (Figure 3b) was generated by a digital elevation model (DEM) of the studied area with a grid resolution of 20 m (see Data and Resource section). For each lithological class, wet (considering groundwater table at 10 m of depth) or dry conditions were assigned. Overlying the slope angle, groundwater, and lithology class maps, it was possible to draw a map of the landslide susceptibility which was finally transformed into the critical acceleration map, k_c , shown in Figure 5a, adopting the simplified method by Wilson and Keefer (1985). According to this approach, in each simulated earthquake, permanent displacements occur or not in a susceptible deposit in those cases in which PGA_S exceeds k_c . In particular, to each susceptibility category, a percentage of map area having a landslide susceptible deposit is computed starting from the values proposed by Wieczorek et al. (1985). Then, such values are used as probabilities of observing landslide at a site, given that PGA_S at the site exceeds k_c (Weatherill et al., 2014). The resulting displacement induced by landslide (PGD_{land}) is finally calculated via the Saygili and Rathje (2008) empirical model; Eq. (3). The model is also characterized by a residual with a standard deviation, $\sigma_{\ln(PGD_{land})}$.

$$\begin{aligned} \ln(PGD_{land}) = & 5.52 - 4.43 \cdot \left(\frac{k_c}{PGA_S}\right) - 20.39 \cdot \left(\frac{k_c}{PGA_S}\right)^2 \\ & + 42.61 \cdot \left(\frac{k_c}{PGA_S}\right)^3 + -28.74 \cdot \left(\frac{k_c}{PGA_S}\right)^4 + 0.72 \\ & \cdot \ln(PGA_S) \end{aligned} \quad (3)$$

Regarding the liquefaction susceptibility map, in the liquefaction-prone areas, basing on the groundwater table depth, the presence and the thickness of wet sand soils and the historical liquefaction events, a liquefaction susceptibility category (SC) was assigned (none, moderate, high, and very high) according to HAZUS procedure, based on the analysis of Youd and Perkins (1978), Figure 5b. As shown, most of the network is not susceptible to liquefaction, limited portions are in the moderate and high susceptibility zones and the very high susceptibility class is of concern only for a small portion of the network between Caserta and Benevento POPs.

Each SC are associated to site specific *liquefaction coefficients*, derived from the empirical models of Liao et al. (1988), as well as *correction factors* that depend on the groundwater depths and the magnitude of the event (see Seed & Idriss, 1982, for further details). The likelihood that an earthquake will be able to trigger liquefaction is then evaluated for each point of the network as a function of these site-specific liquefaction coefficients

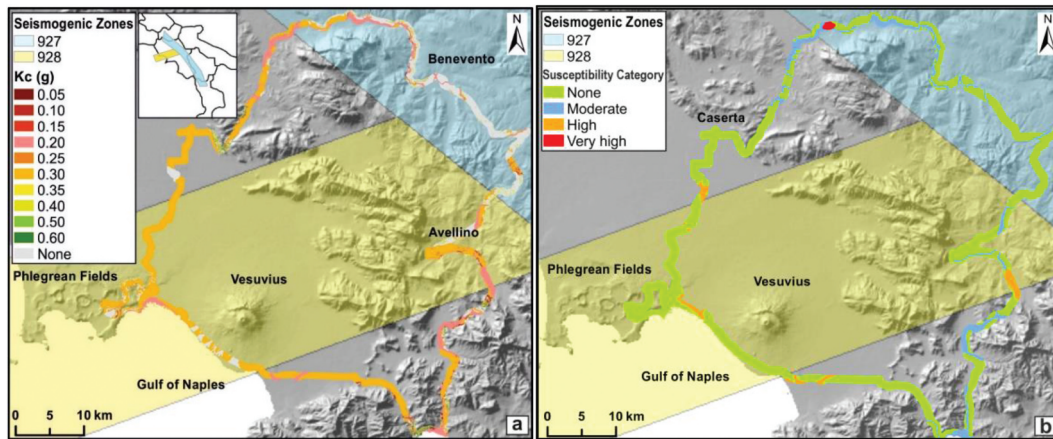


Figure 5. (a) k_c critical acceleration map; (b) liquefaction susceptibility map.

and correction factors. In this basis, liquefaction occurrence is sampled and, if liquefaction occurs, the displacement due to lateral spreading (PGD_{LS}) and the displacement due to settlement (PGD_{SET}) can be estimated. PGD_{LS} is evaluated (in meters) following Eq. (4):

$$PGD_{LS} = 0.0254 \cdot K_{\Delta} \cdot E[PGD(PGA)] \quad (4)$$

where $E[PGD(PGA)]$ is the expected displacement of the ground that depends on the value of the PGA and the SC the point belongs to, and K_{Δ} is a displacement correction term calculated from Seed & Idriss (1982). On the other hand, PGD_{SET} is a characteristic settlement attributed to each susceptibility class (FEMA, 2004) determined via the approach of Tokimatsu and Seed (1987).

5.2. Damage assessment

To assess earthquake-induced damage in each simulation, IMs were related to system component damage via fragility models. Seismic vulnerabilities of both nodes and links are considered in the analyses as described in the following sections.

5.2.1. Damage assessment of nodes

The functionality of the nodes (i.e., POPs) depends on the seismic behavior of the building housing and on the response of the non-structural component; i.e., the rack. The complete loss of functionality of each POP (i.e., no data transmission) has been attributed to: (i) the building collapse (complete damage state), or (ii) the sliding or the overturning of the rack causing malfunction. Thus, if complete damage of the building or overturning of the rack is observed in numerical simulations, the POP is considered failed. This happens when the

simulated PGA_s at the site is larger than at least one of the two PGA values sampled from the building and rack fragility functions.

To identify fragility models, the following information were identified for each building: the building typology, the number of floors, the HAZUS class, and the level of seismic design according to HAZUS (i.e., pre-code, low-code, moderate-code, high-code). As summarized in Table 2, the POP of Naples is a 3 story building with reinforced concrete (RC) shear walls that corresponds, in HAZUS taxonomy, to C2L building type; the POP of Salerno is a single story RC moment frame structure, or C1L; Benevento is a 3 story building made of unreinforced masonry (URM), that is URMM in HAZUS; finally the structure of Caserta is a 3 story RC moment frame with unreinforced masonry infill walls, or C3L.

Buildings fragility functions available in literature were selected through the use of the FRAME software (Petruzzelli & Iervolino, 2014) according to the structural typology, material, number of floors, and seismic code level. The vulnerabilities of the racks were characterized via the fragility functions for acceleration-sensitive non-structural components provided by HAZUS. All the fragility functions adopt PGA as the IM and their parameters (i.e., median and standard deviation of the logarithm) are summarized in Table 3. It is worth noting that rack fragility is always below the corresponding building fragility, except for the case of Benevento POP in which the two fragility functions intersect for a low PGA .

5.2.2. Damage assessment of links

As stated in Section 3.2, links are potentially damaged by both TGD and PGD but a dedicated fragility models for optical cables is, to the authors knowledge, not available. In Esposito et al. (2018), a preliminary study

Table 2. HAZUS (FEMA, 2004) class for the vulnerability characterization of the buildings and of the non-structural components (racks) characterizing each node of the network.

	Naples	Salerno	Benevento	Caserta
Building typology	RC shear walls	RC frame	URM	RC with URM walls
Floors	3	1	3	3
HAZUS Class	C2L	C1L	URMM	C3L
Seismic code	Moderate Code	Moderate Code	Pre-Code	Low Code

was presented adopting a simplified expert-based model to describe possible cable breaks. However, Kongar et al. (2017) analyzed the seismic performance of buried electrical cables of medium voltage network collecting the observed damages caused by the 2010–2011 Canterbury seismic sequence in New Zealand. The study defined the repair rates for buried cables as function of ground deformation due to liquefaction. In fact, cable damages due to *TGD* were estimated as negligible, while no data about landslide effects were available. The results of Kongar et al. (2017) for buried electric cables are adopted here for buried optical cables. Thus, the *RR* is computed according to Eq. (5) in which α is a coefficient that depends on the cable typology (i.e., insulation material within the electrical cable) and PGD_{liq} is the geometric mean of PGD_{SET} and PGD_{LS} . Since none of the considered typologies corresponds to fiber optic cables, two values of α are adopted to discuss its influence on the network performance, $\alpha = 0.26$ and $\alpha = 1.07$, associated to the less and the most vulnerable cable typology, respectively. Moreover, the case of no cable vulnerability, that is, $\alpha = 0$, is also considered in the analyses (Section 6).

$$RR = \alpha \cdot (4.317 \cdot PGD_{liq} - 0.324) \quad (5)$$

As pertaining to landslide, no equivalent relations between PGD_{land} and *RR* are known. Thus, it is here assumed that when the site is interested by landslide, Eq. (5) can be applied substituting PGD_{liq} with PGD_{land} .

Table 3. Fragility functions selected for the building and the rack of each node of the network.

		Naples	Salerno	Caserta	Benevento
IM		PGA	PGA	PGA	PGA
Building	DS	Complete	Complete	DS5	DS5
	Median [g]	0.78	0.78	0.41	7.31
	Standard deviation	0.33	0.33	0.73	2.00
Rack	DS	Moderate	Moderate	Moderate	Moderate
	Median [g]	0.30	0.23	0.17	0.13
	Standard deviation	0.64	0.64	0.64	0.64

5.3. Performance assessment

The seismic performance of the network has been carried out in each run via a capacity analysis, evaluating the capacity of the network expressed in terms of total traffic delivered to each destination, before and after the seismic event. Before proceeding to describe the way in which traffic losses are computed, some characteristics of the main loop of network have to be clarified. Indeed, it was verified that the links are all made of fiber optics with very high capacity (10/100Gpbs), and the number of users of the network is still low. Thus, the capacity of both links and POPs is virtually unbounded and, in the analyses, it is assumed that, after the earthquake, the RIMIC main loop is always able to carry, without delay, also the additional traffic rerouted because of the failure of some other links. It is also assumed that, although each link is constituted by two cables to allow physical-layer mechanisms of failure recovery, in the case of seismic damage, the correlation between damages of the two cables is perfect and the fragility model of Eq. (5) is applied once to the entire link. Moreover, due to the topological simplicity of the analyzed portion of the network, the delay due to the routing-layer mechanisms, is assumed to be zero. In other words, traffic loss is zero if, after the earthquake, POPs are not damaged and damaged links are all located between the same couple of POPs. Finally, it is also assumed that the amount of traffic delivered by each station is variable during the day (as described in the following) but is not modified by the occurrence of the earthquake. In accordance with these hypotheses, the capacity analysis of the network does not require the formulation of flow equations but can be performed as described in the following.

First, the network (considered bi-directional) has been modelled as a graph characterized by the connectivity matrix (*C*) reported in Table 4: the generic element of the matrix at line *s* and column *q*, indicated by $C(s, q)$, is equal to one if the nodes *s* and *q* are directly connected by links, and is zero otherwise.

Being the network bi-directional, the connectivity matrix is symmetrical; zero elements in the matrix correspond to nodes that are not directly connected; i.e., BN-NA and SA-CE. As shown in the connectivity matrix, each node is also connected with itself. This is to handle traffic of links not considered in this simplified topology, but present in the full topology of the network, where secondary loops are attached to each node of the main loop.

From the connectivity matrix, a path matrix (*P*) can be derived; it represents the possibility of any nodes to be connected with any others, even not directly (it can also be derived by the routing tables defined in section

Table 4. Connectivity matrix of RIMIC.

	NA	SA	BN	CE
NA	1	1	0	1
SA	1	1	1	0
BN	0	1	1	1
CE	1	0	1	1

2.1). Thus, in absence of damage, the P matrix derived from C is a unit matrix, i.e., all its elements are equal to one.

A third matrix has to be defined for performance assessment. This is the baseline traffic matrix (T_0) and contains the volumes of traffic exchanged by the nodes; it is based on the following assumptions:

- each row identifies the station from which the traffic is sent; each column the station to which the traffic is addressed;
- nodes deliver the same amount of traffic to the other nodes with the only exception of the node in Naples that is also the gateway to the internet;
- each node sends and receives no traffic towards itself, except Naples (i.e., the one towards the internet).

The baseline traffic matrix is reported in Table 5. This table shows the traffic divided by the total traffic delivered from each station so that the sum of each row is equal to 1 and the total (nondimensional) traffic delivered through the network, defined as $T_{0,tot}$, is equal to 4; each node sends 0.1 traffic units (TUs) towards the others and 0.7 TUs towards the internet (through Naples-POP).

This matrix was defined as a baseline because, in order to account for traffic variation during the day, each element of the baseline matrix is scaled by a factor (a) that takes into account the hour of the day according to the Table 6.

Thus, the elements of the traffic matrix at a particular hour, T_h , are obtained according to Eq. (6):

$$T_h(s, q) = a \cdot T_0(s, q) \quad (6)$$

Table 5. Baseline traffic matrix of RIMIC.

FROM\TO	NA	SA	BN	CE
NA	0.7	0.1	0.1	0.1
SA	0.8	0	0.1	0.1
BN	0.8	0.1	0	0.1
CE	0.8	0.1	0.1	0

Table 6. Numerical values of factor a as a function of the day hours.

Hours	[0; 2[[2; 4[[4; 6[[6; 8[[8; 10[[10; 12[[12; 14[[14; 16[[16; 18[[18; 20[[20; 22[[22; 0[
a	0.15	0.1	0.01	0.08	0.3	0.8	0.95	1	0.92	0.7	0.5	0.2

The sum of each column of T_h represents the traffic delivered to each destination. The sum of all the elements of the matrix is the total traffic ($T_{h,tot}$) delivered to the destinations at a particular hour; thus $T_{h,tot} = a \cdot T_{0,tot}$

After an earthquake, each link and node of the main loop is either considered still working or failed using the vulnerability models described above. Then, the performance of the network is evaluated starting from an updated connectivity matrix, C' , where zero replaces one for broken links. Thus, a new path matrix is computed, P' , accounting for the broken links in C' : if nodes s and q are not connected (directly or not) due to broken links, $P'(s, q) = P'(q, s) = 0$. Moreover, to account for broken nodes, a damage matrix, D , is defined. If no node has failed, all the elements of D are equal to one (it is a unit matrix); on the other hand, assuming that the node s has failed during the earthquake, the elements of the line s and column s are all equal to zero, that is: $D(s, i) = D(i, s) = 0$ for $i = 1, 2, \dots, 4$ (the other elements remain equal to one if the other nodes are undamaged).

The updated post-event traffic matrix, T_h' , is computed multiplying each element of T_h by the corresponding element of P' and D , as shown in Eq. (7):

$$T_h'(s, q) = P'(s, q) \cdot D(s, q) \cdot T_h(s, q). \quad (7)$$

The sum of the elements of T_h' , indicated as $T_{h,left}$, is the traffic delivered after the earthquake. Thus, the amount of total traffic that cannot be delivered, that is, the traffic loss, $T_{h,lost}$, is equal to $T_{h,tot} - T_{h,left}$. The metric chosen as PI for the case study is the ratio of traffic loss to the total baseline traffic of the network, that is $T_{0,tot}$; in terms of equation:

$$PI = T_{h,lost} / T_{0,tot} = (T_{h,tot} - T_{h,left}) / T_{0,tot}. \quad (8)$$

6. Results and discussion

The performances of the network were analyzed via Monte Carlo simulations performed according the flow-chart of Figure 6 that summarizes the simulation procedure described in Sections 5.1, 5.2 and 5.3. Results discussed in this section are obtained through one hundred fifty thousand simulations (i.e., one hundred fifty thousand simulated earthquakes). Indeed, it has been verified that increasing the number of simulations does not produce significant differences in the results.

Once the chosen PI is computed for each simulated scenario by one seismic source area, the empirical complementary cumulative distribution function (CCDF) of PI conditional to the occurrence of a generic earthquake of the source area (i.e., an earthquake of unknown magnitude and location) can be derived. Then, the annual exceedance rate of the PI due to each source is computed multiplying the occurrence rate of earthquakes on the seismic source (see Table 1), with the corresponding CCDF of PI; i.e., the distribution of the traffic loss given the occurrence of an earthquake on that source. Thus, the annual exceedance rate of the network, λ_{PI} , is the sum of those related to each seismic source.

According to section 5.2, the simulations were repeated considering three vulnerability functions for cables represented by three values of the α parameter

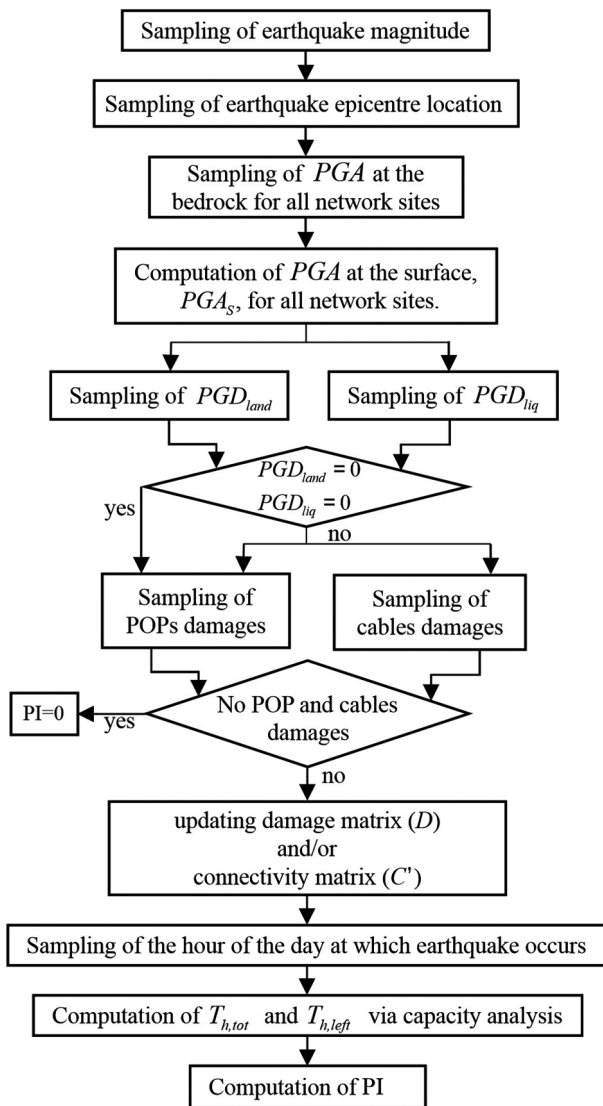


Figure 6. Flowchart of a generic run of the Monte Carlo simulation.

of Eq. (5): α equal to zero, 0.26 and 1.07 that correspond to zero, low, and high cables vulnerability, respectively. The annual exceedance rates as a function of PI are shown in Figure 7.

The three curves show that the cable fragilities have minor effects on the network performance. This is for a number of reasons: (i) according to the adopted model, cables are not susceptible to transient ground displacements; (ii) permanent ground displacements, to which cables are vulnerable, may be produced by liquefaction but the most of the network is located on sites with no liquefaction susceptibility (see Figure 5b); (iii) the critical acceleration map in Figure 5b shows that, for the most part of the network, a PGA_s higher than 0.30 g is required for triggering landslides (a significant value for the Italian seismic context); (iv) as discussed, when ruptures of cables are located between only one couple of POPs, traffic loss due to cable fails is zero.

Figure 7 also shows that the curves of annual loss rates have one main drop for PI equal to 0.325. This value can be easily computed from Eqs. (7) and (8) assuming that only one POP (among Salerno, Caserta or Avellino) fails (or is isolated by cables failure) in a daily hour corresponding to $a = 1$ (in such case, $T_{h,left} = 2.7$ and $T_{h,lost} = 1.3$). The exceedance rate associated to this PI is between about $9.45E-4$ and $8.12E-04$ (for $\alpha = 1.07$ and $\alpha = 0$, respectively), that is, the mean interarrival time between two subsequent earthquakes causing such a PI is between 1058 and 1232 years.¹ The comparison of these numbers with the earthquake return period on the sources (2.4 years according to Section 5.1) suggests a relatively good performance of the network with respect to the seismic threat. In fact, Figure 7 shows minor drops occurring for PI values lower than 0.325: they are due to the already discussed damage scenario but simulated in other hours and, consequently, corresponding to lower values of a and lower PI.

In order to discuss which POP mostly contributes to the traffic loss, the conditional probability of observing at least the failure of one POP given that $PI > 0$, $P_f[POP|PI > 0]$, is reported in Figure 8 (i.e., the number of simulated scenarios in which at least one POP fails, divided by the number of scenarios with $PI > 0$). As shown, the POP mostly contributing to losses is Benevento, the closest to the Irpinia region, which is the most seismically hazardous area in the region.

As described in section 5.3, traffic loss can be caused by cable failures if failures are located between more than one couple of POPs: one possible case is cable failures cause the isolation of one POP from the rest of the network. This is analyzed in

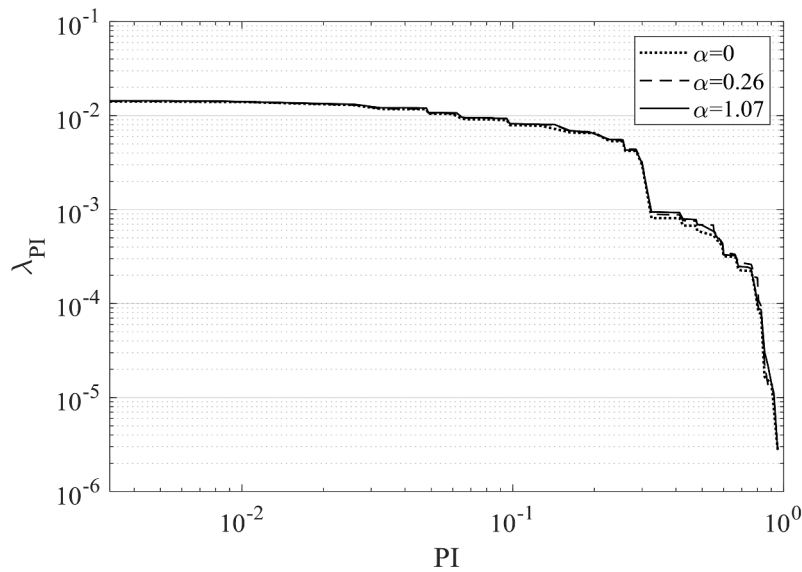


Figure 7. Annual rate of exceedance of PI computed according to the three hypotheses on cables fragilities.

Figure 9 where the probability of observing the isolation of at least one POP given $PI > 0$, $P_{is}[POP|PI > 0]$, is shown. Such a probability is higher for the POP of Benevento meaning that the conditional probability of observing at least one cable rupture between Benevento and Caserta and between Benevento and Salerno is the highest. Figure 9 also confirms that results are slightly influenced by the model of cables fragility (i.e., the value of α).

7. Conclusion

The probabilistic seismic risk assessment of a data communication network was discussed in the study. The work was framed in the broader topic of performance-based assessment of spatially distributed infrastructure

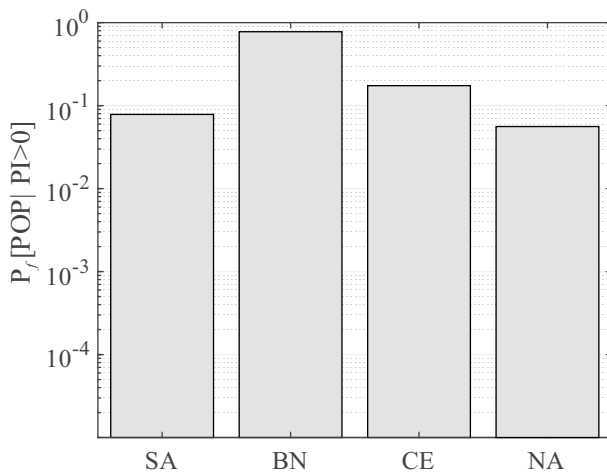


Figure 8. Failure probability of at least one POP conditional to $PI > 0$.

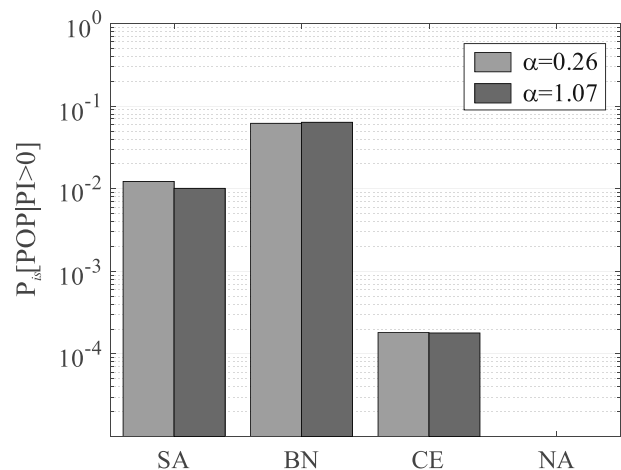


Figure 9. Probability of observing one POP isolated from the rest of the network, conditional to $PI > 0$.

and lifelines, which is the focus of a significant deal of current research. The considered network is the main loop of the RIMIC network connecting the universities in the Campania region, a seismically active territory in Italy.

The Monte Carlo simulation required to carry out the seismic risk assessment was illustrated step-by-step and implemented in an object-oriented framework developed in previous research effort. In fact, the analysis' framework, which targeted the traffic loss assessment via a capacitive assessment of the data infrastructure after seismic events, was applied to a real test case.

For the purposes of the analysis, the seismological, geological, and geotechnical features of the region were characterized, requiring engineering seismology and

engineering geology efforts. Subsequently, the vulnerability of the physical assets of the network was modelled. Finally, the performance of the network in damaged conditions was carried out choosing as PI, the ratio of the traffic loss after the seismic event with respect to the total (maximum) traffic delivered before the earthquake.

Results, in terms of annual rates of losses, are discussed referring to significant damage scenarios. A relatively resilient performance of the network to seismic action is shown together with a minor effect of cable fragilities on the network performance. Results are also disaggregated in order to quantify the probability that traffic loss is due to (i) the failure or (ii) the isolation of a specific POP. Both results identified the POP of Benevento as the one that contributes the most to the traffic losses.

Note

1. Seismic damage accumulation on the network due to seismic sequence or network damage due to other actions (e.g. aging) are neglected in the analyses.

Acknowledgments

This work was developed within the GRISIS – *Gestione dei Rischi e Sicurezza delle Infrastrutture a Scala regionale*, funded by Regione Campania – POR FESR 2014-2020.

Disclosure statement

No potential conflict of interest was reported by the author(s).

Funding

This work was supported by the Regione Campania [GRISIS project - POR FESR 2014-2020].

Notes on contributors

Simona Esposito is senior property treaty underwriter at Swiss RE.

Alessio Botta is assistant professor of Computer Engineering at the University of Napoli Federico II.

Melania De Falco has a Ph.D. in management and development of agricultural and forest resources.

Adriana Pacifico is a Ph.D. candidate in Structural Engineering, Geotechnics and Seismic Risk at the University of Napoli Federico II.

Eugenio Chioccarelli is senior researcher in Structural Engineering at the University of Reggio Calabria.

Antonio Pescapè is full professor at the Department of Electrical Engineering and Information Technology of the University of Napoli Federico II

Antonio Santo is associate professor of Engineering Geology at the University of Napoli Federico II.

Iunio Iervolino is full professor of Structural Engineering at the University of Napoli Federico II.

ORCID

Alessio Botta  <http://orcid.org/0000-0002-3365-1446>

Melania De Falco  <http://orcid.org/0000-0002-6904-0946>

Eugenio Chioccarelli  <http://orcid.org/0000-0002-8990-3120>

Antonio Pescapè  <http://orcid.org/0000-0002-0221-7444>

Iunio Iervolino  <http://orcid.org/0000-0002-4076-2718>

Data and Resources

Geological data are provided via a 1:100.000 scale maps provided by ISPRA (<http://www.isprambiente.gov.it/>, last accessed 03/08/2020). The digital elevation model is available at <http://www.mais.sinanet.isprambiente.it>, last accessed 03/08/2020. The rest of the data is from the listed references.

References

- Adachi, T., & Ellingwood, B. R. (2008). Serviceability of earthquake-damaged water systems: effects of electrical power availability and power backup systems on system vulnerability. *Reliability Engineering and System Safety*, 93(1), Elsevier, 78–88. doi:10.1016/j.res.2006.10.014
- Argyroudis, S., Selva, J., Gehl, P., & Pitilakis, K. (2015). Systemic seismic risk assessment of road networks considering interactions with the built environment. *Computer-Aided Civil and Infrastructure Engineering*, 30(7), 524–540. doi:10.1111/mice.12136
- Barani, S., Spallarossa, D., & Bazzurro, P. (2009). Disaggregation of probabilistic ground motion hazard in Italy. *Bulletin of the Seismological Society of America*, 99(5), 2638–2661. doi:10.1785/0120080348
- Bischof, Z. S., Otto, J. S., & Bustamante, F. E. Distributed systems and natural disasters: bittorrent as a global witness. In *Proceedings of the Special Workshop on Internet and Disasters*, December, Tokyo, Japan, Article No. 4. doi:10.1145/2079360.2079364.
- Bommer, J. J., Akkar, S., & Drouet, S. (2012). Extending ground-motion prediction equations for spectral accelerations to higher response frequencies. *Bulletin of Earthquake Engineering*, 10(2), 379–399. doi:10.1007/s10518-011-9304-0
- Cavaliere, F., Franchin, P., Buriticá Cortés, J. A. M., & Tesfamariam, S. (2014a). Models for seismic vulnerability analysis of power networks: Comparative assessment. *Computer-Aided Civil and Infrastructure Engineering*, 29(8), 590–607. doi:10.1111/mice.12064
- Cavaliere, F., Franchin, P., & Pinto, P. E. (2014b). Application to selected transportation and electric networks in Italy. *Geotechnical, Geological and Earthquake Engineering* (301–330). Kluwer Academic Publishers 10.1007/978-94-017-8835-9_10

- Cetinkaya, E. K., & Sterbenz, J. P. G. (2013). A taxonomy of network challenges. In *Proceedings of the 9th International Conference on Design of Reliable Communication Networks (DRCN)*, Budapest, Hungary, 322–330.
- Chang, L., Elnashai, A. S., Billie, F., & Spencer, J. (2012). Post-earthquake modelling of transportation networks. *Structure and Infrastructure Engineering*, 8(10), 893–911. doi:10.1080/15732479.2011.574810.
- Chang, L., & Wu, Z. (2011). Performance and reliability of electrical power grids under cascading failures. *International Journal of Electrical Power and Energy Systems*, 33(8), 1410–1419. doi:10.1016/j.ijepes.2011.06.021
- Chioccarelli, E., Cito, P., Iervolino, I., & Giorgio, M. (2019). REASSESS V2.0: Software for single- and multi-site probabilistic seismic hazard analysis. *Bulletin of Earthquake Engineering*, 17(4), Springer Netherlands, 1769–1793. doi:10.1007/s10518-018-00531-x
- Cho, K., Pelsser, C., Bush, R., & Won, Y. (2011). The Japan Earthquake: the impact on traffic and routing observed by a local ISP. In *Proceedings of the Special Workshop on Internet and Disasters*, December, Tokyo, Japan.
- Cornell, C. A., & Krawinkler, H. (2000). Progress and challenges in seismic performance assessment. *PEER Center News 3*. CA, USA: Pacific Earthquake Engineering Center; University of California. <https://apps.peer.berkeley.edu/news/2000spring/performance.html>.
- D'onofrio, A., Mastrangelo, A., Penna, A., Santo, A., & Silvestri, F. (2013). Predicted vs. Observed Performances of the L'Aquila Gas Network during the 2009 Earthquake. *Rivista Italiana di Geotecnica*, 47(4), 38–54.
- Duenas-Osorio, L., Craig, J. I., & Goodno, B. (2007). Seismic response of critical interdependent networks. *Earthquake Engineering and Structural Dynamics*, 36(2), 285–306. doi:10.1002/eqe.626
- Esposito, S., Botta, A., & De Falco, M. (2018). Seismic risk analysis of data communication networks: a feasibility study. In *Proceedings of the 16th European Conference on Earthquake Engineering*, Thessaloniki, Greece.
- Esposito, S., Iervolino, I., d'Onofrio, A., Santo, A., Cavalieri, F., & Franchin, P. (2015). Simulation-based seismic risk assessment of gas distribution networks. *Computer-Aided Civil and Infrastructure Engineering*, 30(7), 508–523. doi:10.1111/mice.12105
- Esposito, S., & Iervolino, I. (2011). PGA and PGV spatial correlation models based on European multievent datasets. *Bulletin of the Seismological Society of America*, 101(5), 2532–2541. doi:10.1785/0120110117
- EUROCODE 8. (2003). Design of structures for earthquake resistance. Part 1: General Rules, Seismic Actions and Rules for Buildings.
- FEMA. (2004). *Multi-Hazard Loss Estimation Methodology: Earthquake Model: HAZUS MR4, Technical Manual*.
- Forte, G., Fabbrocino, S., de Santucci Magistris, F., Silvestri, F., & Fabbrocino, G. (2015). Earthquake Triggered Landslides: The Case Study of a Roadway Network in Molise Region (Italy). In *Proceedings of the Engineering Geology for Society and Territory 2: Landslide Processes, XII International Symposium IAEG*, Torino, Italy, Vol. 2, 765–768. doi:10.1007/978-3-319-09057-3_129
- Forte, G., Fabbrocino, S., Fabbrocino, G., Lanzano, G., de Santucci Magistris, F., & Silvestri, F. (2017). A geolithological approach to seismic site classification: An application to the Molise region (Italy). *Bulletin of Earthquake Engineering*, 15(1), Springer Netherlands, 175–198. doi:10.1007/s10518-016-9960-1
- Franchin, P., & Cavalieri, F. (2013). *Seismic Vulnerability Analysis of a Complex Interconnected Civil Infrastructure*. Handbook of Seismic Risk Analysis and Management of Civil Infrastructure Systems. doi:10.1533/978085709864.4.465
- Fukuda, K., Aoki, M., Abe, S., Ji, Y., Koibuchi, M., Nakamura, M., Yamada, S., & Urushidani, S. (2011). Impact of Tohoku Earthquake on R&E Network in Japan. In *Proceedings of the Special Workshop on Internet and Disasters*, December, Tokyo, Japan.
- Gutenberg, B., & Richter, C. F. (1944). Frequency of Earthquakes in California. In *Bulletin of the Seismological Society of America*, 34(4), 185–188. doi:10.1785/bssa0340040185.
- Jayaram, N., & Baker, J. W. (2009). Correlation model for spatially distributed ground motion intensities. *Earthquake Engineering and Structural Dynamics*, 38(15), 1687–1708. doi:10.1002/eqe.922
- Kiremidjian, A., Moore, J., Fan, Y. Y., Yazlali, O., Basoz, N., & Williams, M. (2007). Seismic risk assessment of transportation network systems. *Journal of Earthquake Engineering*, 11(3), 371–382. Taylor & Francis Group. doi:10.1080/13632460701285277
- Kitamura, Y., Lee, Y., Sakiyama, R., & Okamura, K. (2007). Experience with restoration of asia pacific network failures from taiwan earthquake. *IEICE Transactions on Communications E90-B (11)*, 3095–3103. doi:10.1093/iet-com/e90-b.11.3095.
- Kongar, I., Giovinazzi, S., & Rossetto, T. (2017). Seismic performance of buried electrical cables: Evidence-based repair rates and fragility functions. *Bulletin of Earthquake Engineering*, 15(7), Springer Netherlands, 3151–3181. doi:10.1007/s10518-016-0077-3
- Kramer, S. L. (1996). *Geotechnical earthquake engineering*. Upper Saddle River, New Jersey 07458: Prentice-Hall, Inc.
- Lanzano, G., Salzano, E., de Santucci Magistris, F., & Fabbrocino, G. (2014). Seismic vulnerability of gas and liquid buried pipelines. *Journal of Loss Prevention in the Process Industries*, 28(April), 72–78. Elsevier Ltd. doi:10.1016/j.jlp.2013.03.010
- Leelardcharoen, K. (2011). Interdependent Response of Telecommunication and Electric Power System to Seismic Hazard. Ph.D. Thesis, Georgia Institute of Technology.
- Liao, S. S. C., Veneziano, D., & Whitman, R. V. (1988). Regression models for evaluating liquefaction probability. *Journal of Geotechnical Engineering*, 114(4), 389–411. doi:10.1061/(ASCE)0733-9410(1988)114:4(389)
- Liu, Y., Luo, X., Chang, R. K. C., & Su, J. (2012). Characterizing Inter-Domain Rerouting after Japan Earthquake. In *Proceedings of the 11th International IFIP TC 6 Networking Conference*, Prague, Czech Republic.
- Loth, C., & Baker, J. W. (2013). A spatial cross-correlation model of spectral accelerations at multiple periods. *Earthquake Engineering and Structural Dynamics*, 42 (June), 397–417. doi:10.1002/eqe
- Meletti, C., Galadini, F., Valensise, G., Stucchi, M., Basili, R., Barba, S., Vannucci, G., & Boschi, E. (2008). A Seismic Source Zone Model for the Seismic Hazard Assessment of the Italian Territory. *Tectonophysics*, 450(1–4), 85–108. doi:10.1016/j.tecto.2008.01.003

- Ningxiong, X., Guikema, S.D., Davidson, R.A., Nozick, L.K., Cagnan, Z., & Vaziri, K. (2007). Optimizing Scheduling of Post-Earthquake Electric Power Restoration Tasks. *Earthquake Engineering and Structural Dynamics* 36, 265–284. doi:10.1002/eqe.
- Nuti, C., Rasulo, A., & Vanzi, I. (2009). Seismic Safety of Network Structures and Infrastructures. *Structure and Infrastructure Engineering*, 6(1–2), 95–100. doi:10.1080/15732470802663813
- O'Rourke, T. D., & Palmer, M. C. (1996). Earthquake Performance of Gas Transmission Pipelines. *Earthquake Spectra*, 20(3), 493–527. doi:10.1193/1.1585895
- Omidvar, B., Hojjati Malekshah, M., & Omidvar, H. (2014). Failure risk assessment of interdependent infrastructures against earthquake, a petri net approach: case study-power and water distribution networks. *Natural Hazards*, 71 (April), 1971–1993. doi:10.1007/s11069-013-0990-6
- Patacca, E., & Scandone, P. (2007). Geology of the Southern Apennines. *Bollettino Della Società Geologica Italiana, Special Is*, (7), 75–119.
- Petersen, M. D., Dawson, T. E., Chen, R., Cao, T., Wills, C. J., Schwartz, D. P., & Frankel, A. D. (2011). Fault displacement hazard for strike-slip faults. *Bulletin of the Seismological Society of America*, 101(2), 805–825. doi:10.1785/0120100035
- Petruzzelli, F., & Iervolino, I. (2014). FRAME V.1.0: A rapid fragility-based seismic risk assessment tool. In *Proceedings of the Second European Conference on Earthquake Engineering and Seismology, 2ECEES, - Istanbul, Turkey*.
- Pitilakis, K., Franchin, P., Khazai, B., & Wenzel, H. (2014). SYNER-G: systemic seismic vulnerability and risk assessment of complex urban, utility, lifeline systems and critical facilities.: Methodology and Applications. *Geotechnical, Geological and Earthquake Engineering*. Vol. 31. Springer. doi:10.1007/978-94-017-8835-9.
- Poljanšek, K., Bono, F., & Gutiérrez, E. (2012). Seismic risk assessment of interdependent critical infrastructure systems: The case of European gas and electricity networks. *Earthquake Engineering and Structural Dynamics*, 41(1), 61–79. John Wiley and Sons Ltd. doi:10.1002/eqe.1118
- Saygili, G., & Rathje, E. M. (2008). Empirical predictive models for earthquake-induced sliding displacements of slopes. *Journal of Geotechnical and Geoenvironmental Engineering*, 134(6), 790–803. doi:10.1061/(ASCE)1090-0241(2008)134:6(790)
- Seed, H. B., & Idriss, I. M. (1982). Ground Motions and Soil Liquefaction During Earthquakes. *Earthquake Engineering Research Institute*, Oakland, California.
- Stucchi, M., Meletti, C., Montaldo, V., Crowley, H., Calvi, G. M., & Boschi, E. (2011). Seismic hazard assessment (2003 – 2009) for the Italian building code. *Bulletin of the Seismological Society of America*, 101(4), 1885–1911. doi:10.1785/0120100130
- Tang, A. K. (2008). *The Shake out scenario, supplemental study: telecommunications*. U.S. Geological Survey Open File Report. Pasadena, California.
- Tang, A. K. (2014). *Building telecommunication system resilience – lessons from past earthquakes*. In *Proceedings of the 6th China-Japan-US Trilateral Symposium on Lifeline Earthquake Engineering*. ASCE, Vol. 30. doi:10.1061/9780784413234.010.
- TCLEE, Technical Council on Lifeline Earthquake Engineering. (2011). *Report of the 11 march 2011 Mw 9.0 Tohoku, japan earthquake and tsunami*. Edited by A. K. Tang & C. Edwards
- TCLEE, Technical Council on Lifeline Earthquake Engineering. (2012). *Christchurch, New Zealand Earthquake Sequence of Mw 7.1 September 04, 2010 Mw 6.3 February 22, 2011, Mw 6.0 June 13, 2011: Lifeline Performance*. Edited by J. Eidinger & A. K. Tang
- Tokimatsu, K., & Seed, H. B. (1987). Evaluation of settlement in sands due to earthquake shaking. *Journal of Geotechnical and Geoenvironmental Engineering*, 113(8), 861–878. doi:10.1061/(ASCE)0733-9410(1987)113:8(861)
- Vanzi, I. (2000). Structural upgrading strategy for electric power networks under seismic action. *Earthquake Engineering and Structural Dynamics*, 29(7), 1053–1073. doi:10.1002/1096-9845(200007)29:7<1053::AID-EQE954>3.0.CO;2-X
- Weatherill, G., Esposito, S., Iervolino, I., Franchin, P., & Cavalieri, F. (2014). Framework for Seismic Hazard Analysis of Spatially Distributed Systems. *Geotechnical, Geological and Earthquake Engineering* 31, 57–88. doi:10.1007/978-94-017-8835-9_3.
- Wieczorek, G. F., Wilson, R. C., & Harp, E. L. (1985). Map of Slope Stability during Earthquakes in San Mateo County. In *U.S. Geological Survey Miscellaneous Investigations, California, Map I-1257-E, Scale 1:62,500*. doi:10.3133/i1257E.
- Wilson, R. C., & Keefer, D. K. (1985). Predicting Areal Limits of Earthquake Induced Landsliding. In J. I. Ziony (Ed.), *Evaluating Earthquake Hazards in the Los Angeles Region*, U.S. Geological Survey Professional Paper, 1360, 317–345.
- Youd, T. L., & Perkins, D. M. (1978). Mapping Liquefaction-Induced Ground Failure Potential. *ASCE Journal of Geotechnical Engineering Division*, 104(GT4), 433–346. doi:10.1061/AJGEB6.0000612